Solution-Processable High-Purity Semiconducting SWCNTs for Large-Area Fabrication of High-Performance Thin-Film Transistors

Jianting Gu, Jie Han, Dan Liu, Xiaoqin Yu, Lixing Kang, Song Qiu, Hehua Jin, Hongbo Li, Qingwen Li,* and Jin Zhang*

Semiconducting single-walled carbon nanotubes (s-SWCNTs) with tunable bandgap and high mobility show great promise in field-effect transistors,[1] intergrated circuit chips,[2] Infrared-based detectors,[3] and flexible sensors,[4] etc. In particular, application of high-purity s-SWCNTs in thin-film transistors (TFTs) has gained intense interest recently on account of growing requirement for low-cost and flexible thin film display techniques for smart phones and TVs, etc.[5] Rational and scalable fabrication of s-SWCNT assemblies between electrodes with high purity, uniformity, and controlled density is crucial for achieving large-area and high-performance TFT-based arrays and circuits. However, due to their subtle difference in structure, separating s-fraction from SWCNT mixture without metallic tubes and meanwhile assembling them on surface with high density are still challenging so far not only for direct chemical vapor deposition (CVD) growth but also for wet chemical separation approaches. The reported purity of s-SWCNTs can be achieved around 95% through in situ CVD growth, since the precise control of catalyst size and component is extremely hard under high temperatures.[6] In contrast, harvesting s-SWCNT via selective dispersion and fractionation has become more competitive due to its simplicity, scalability, and promising control on its purity and assembly on surface.[7]

s-SWCNTs can be effectively sorted from raw SWCNT materials through different wet chemical approaches. Assisted by surfactants, density gradient ultracentrifugation,[8] electrophoresis,[9] gel column chromatography,[10] and aqueous two phases extraction[11] have been demonstrated to be effective in enriching the s-SWCNTs in aqueous solutions with purity up to 99%.[12] Unfortunately, the presence of excessive residual surfactants upon aggregation on surface heavily hindered the charge transport and dramatically degraded the performance of devices.[7c,13] On the contrary, selective dispersion of s-SWCNTs assisted by conjugated molecules in organic solvents has greatly stimulated the progress in device fabrication, with the mobility and on–off ratio of TFT devices improved up to 300 $cm^2\ V^{-1}\ s^{-1}$ and 10^8.[14] This method tends to show the advantages of low manufacturing cost, high scalability, and easy processability. However, different structures of conjugated molecules, usually consisting of different skeletons and side chains, may lead to different interaction with or wrapping along the s-SWCNTs, consequently enabling the sorted solution with different yield and purity.[15] For instance, poly[(9,9-dioctylfluorenyl-2,7-diyl)] (PFO), seems more favorable for sorting the s-SWCNTs with diameter <1.1 nm,[16] however, it becomes more selective to large-diameter s-SWCNTs (1.2–1.4 nm) when tuning its pristine structure with long of alkyl side chain (such as poly[(9,9-didodecylfluorenyl-2,7-diyl)])[16a] or introduction of electron-rich subunits (such as poly[(9,9-dioctylfluorenyl-2,7-diyl)-co-bipyridine] (PFBP)).[17] As large-diameter SWCNTs are more desired for CNT-based electronics devices due to their smaller Schottky barriers and fewer defects,[18] designing molecues for selective harvesting of the s-SWCNTs with diameter >1.3 nm and purity higher than 99% are currently a challenging topic but significant for the fabrication of large-area high-performance TFT devices.

Herein, we demonstrated a new linear homopolymer poly[9-(1-octylonoyl)-9H-carbazole-2,7-diyl], noted as PCz, which was simple to be synthesized but tended to show superior selectivity for large-diameter s-SWCNTs (1.4–1.6 nm) with sorted purity up to 99.9% under a mild ultrasonic and centrifugation condition. The presence of N—C bonds in

J. Gu, J. Han, X. Yu, L. Kang, S. Qiu, H. Jin, H. Li, Prof. Q. Li
Key Laboratory of Nanodevices and Applications
Suzhou Institute of Nanotech and Nano-bionics
Chinese Academy of Science
Suzhou 215123, China
E-mail: sqiu2010@sinano.ac.cn; qwli2007@sinano.ac.cn
J. Gu, L. Kang
University of Chinese Academy of Sciences
Beijing 100049, China
D. Liu, Prof. J. Zhang
Center for Nanochemistry
Beijing National Laboratory for Molecular Sciences
Key Laboratory for the Physics and Chemistry of Nanodevices
State Key Laboratory for Structural Chemistry of Unstable and Stable Species
College of Chemistry and Molecular Engineering
Peking University
Beijing 100871, P. R. China

DOI: 10.1002/smll.201600398

www.MaterialsViews.com

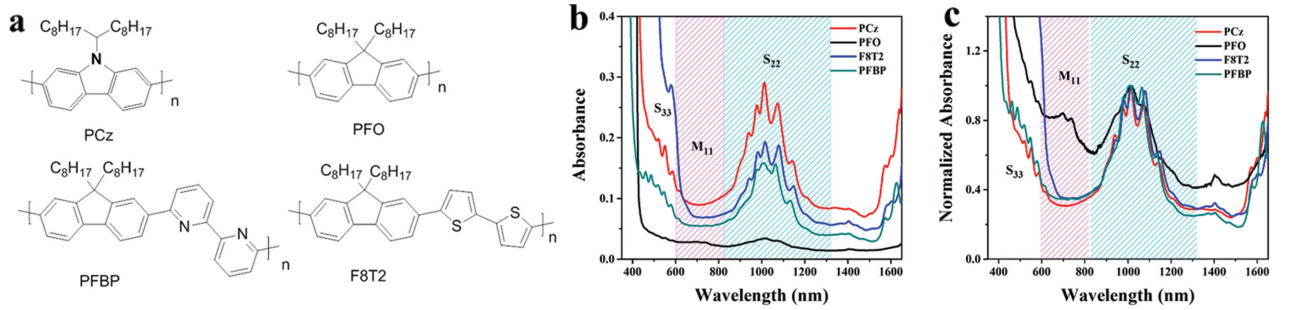

Figure 1. a) The chemical structure of the new customized polycarbazole (PCz), polyfluorenes (PFO), PFBP, and F8T2. b) The absorption spectra and c) normalized absorption spectra of the samples extracted by PCz, PFO, PFBP, F8T2. The spectra were normalized to the peak at around 1012 nm.

PCz enabled the sorted s-SWCNT solution to be stable at a high concentration, and liable to form uniform s-SWCNT networks on wafer-scale SiO_2/Si substrates. To confirm this efficiency, 300 thin-film transistors were fabricated on a 2 in. wafer using a simple dip-coating process. None of the TFTs were failed. The devices exhibited excellent performance with mobility of 28–67.5 $cm^2 V^{-1} s^{-1}$ and 80% of which showed on–off ratios up to 10^6 when the channel lengths (L) were set from 5 to 50 μm, revealing the significant role of PCz in the sorting of ultrahigh-purity s-SWCNTs and scalable fabrication of SWCNT based TFTs.

Different from the previously reported PFO, which were more sensitive to the separation of small-diameter s-SWCNTs (<1.1 nm), we proposed the introduction of N-doped and 1-octylonoyl as lateral chain (**Figure 1**a) to enhance the electron delocalization of PFO conjugated backbone and modify its rigidity and steric hindrance when wrapping along nanotubes. In the pristine PFO structure, a C bridge atom is sp^3 hybridized and therefore an asymmetric tetrahedral configuration is more favorable, in which the two alkyl chains prefer to adjust themselves perpendicular to the conjugated plane, making the SWCNT wrapping more difficult (low yield) and favorable for thin tubes. However, in our new molecular design, the introduction of an electron-rich N bridge atom between alkyl chain and one carbazole unit tends to favor the pristine PFO with a significant dipole moment and energy gap variation,[19] and accordingly affects its interaction with nanotubes. As shown in Figure S1 (Supporting Information), the N-bridge atom in a PCz unit tends to show sp^2 hybridization with a lone pair of electrons and a planar geometry. As a result, in comparison with pure PFO molecule, the introduction of N—C bond between the carbazole unit and the two long octyl chains leads to a torsional degree of freedom (Figure S1, Supporting Information), enabling the molecule to be more flexible and adaptive when interacting with carbon nanotube.

Figure 1a shows the structural comparison between PCz and three widely investigated PFO derivates. In order to make clear the uniqueness and efficiency of PCz, we chose PFO, PFBP, and poly[(9,9-dioctylfluorenyl-2,7-diyl)-co-bithiophene] (F8T2) as reference, respectively, and evaluated their dispersion and sorting efficiency using adsorption spectroscopy. The basic structural properties of these polymers including molecular weight and melting points characterization data were listed in Table S1 (Supporting Information). PFBP and F8T2, with pyridine and thiophene introduced into conjugated skeleton have been reported to be highly effective for dispersing and sorting SWCNTs, and the as-fabricated network TFT devices showed better performance (on–off ratio higher than 10^6 and the mobility up to 40 $cm^2 V^{-1} s^{-1}$) compared to those derived from other reported polyfluorene derivatives.[17,20]

Figure 1b shows the ultraviolet–visible–near infrared (UV–vis–NIR) absorption curves of the sorted s-SWCNT solutions derived from PCz and the other three PFO derivatives, respectively. The background interference can be neglected in all the NIR absorption spectra as the charateristic absorption bands of PCz and three PFO derivates are dominantly located from 350 to 500 nm. It can be clearly seen that under the same ultrasonic and centrifugation procedure, PFO leads to a weak absorption from 820 to 1350 nm which corresponds to S22 band, and a relatively strong absorption assigning to M11 band. Differently, PCz directed nanotube dispersion exhibits the highest absorption peak intensity around 1010 nm that is much higher than the PFO derivates. If comparing PCz with PFBP and F8T2, all of these polymers possess heteroatom dopants in either skeleton or side chains, showing the selectivity enhancement on s-SWCNTs but with a slight difference on diameter distribution. It is more likely inferred that the introduction of heteroatoms in the conjugated skeletons is beneficial for their selective π–π stacking interaction with s-SWCNTs. Moreover, it is also revealed that PCz, which has a N-bridge atom inserted between carbazole and alkyl chains as well as an induced obvious configration alternation, exhibits greatly improved dispersion selectivity than pristine PFO. With respect to PFBP which has N-rich pyridine coupled with PFO skeleton, PCz also presents an enhanced dispersion ability and different preference on s-SWCNT diameter, probably indicating that the conjugated skeleton induced π–π stacking interaction and steric hindrance are both critical for s-SWCNT sorting. To further compare the purities of the four sorted s-SWCNT solutions, all absorption spectra were rescaled and shown in Figure 1c. Based on the ratios of the absorbance of the highest peak in the S22 region and the lowest peak in the M11 region, we can roughly evaluate the purities of s-SWCNTs derived from different polymers. It is revealed that PCz leads to the highest ratio (>3), much higher than PFO while slightly higher than PFBP and F8T2. As PCz displays a valley of the absorption

curve as deep as PFBP and F8T2 in the M11 region, it is hard to further compare and evaluate their purity degrees from the absorption spectra, as the pristine absorption of free polymers and the resolution of the absorption spectrum may interfere the M11 bands.

Micro-Raman spectroscopy is helpful as side evidence to semiquantitatively evaluate the purity of SWCNTs. By scanning the sample on surface, we can measure and map out the radial-breathing-mode (RBM) spectra of the sorted s-SWCNT films to further elucidate the enrichment purity of s-SWCNTs.[21] The s-SWCNT network films were prepared by submerging the Si substrate in the three kinds of nanotube solutions for 12 h without any further purification, i.e., free polymers were codeposited with s-SWCNTs. **Figure 2** shows the as-deposited networks and scanning Raman results derived from the three polymers, respectively. In practice, G^- and G^+ peaks are a useful indicator to estimate the relative content of m/s SWCNTs.[22] Raman spectra of the sorted and unsorted SWCNTs were measured under 633 and 785 nm laser excitation (Figure S2, Supporting Information). During the noise floor and the too low concentration of residual m-SWCNTs, no obvious G^- signal of metallic tubes were measured in these three samples under 633 nm laser excitation. However, under 785 nm laser excitation, the nuances of purity among these samples were observed. Under 785 nm laser excitation, only metallic signatures in the range of 130–180 cm^{-1} were observed in the RBM bands of pristine SWCNTs in toluene and no semiconducting signatures were measured (Figure S2, Supporting Information). As a result, statistic estimation of emergence probability of m-SWCNTs can be roughly used to evaluate the purity of s-SWCNTs.

Figure 2b,e,h shows the RBM mappings of the three kinds of s-SWCNT films. The network films with an area 10×10 μm^2 were proximately composed of around 3000 tubes and scanned under 785 nm laser excitation. The intensity mappings were performed by a RBM window from 130 to 180 cm^{-1} and the representative spectra were extracted at the highlight positions (Figure 2c,f,i). From Figure 2f, it can be seen that RBM peaks centered at 154 cm^{-1} (correspond to m-SWCNT) are clearly observed in the mapping spectra of PFBP. Since the diameter of the laser spot is 0.5 μm and the average tube length is 1–2 μm, if identical spectra are collected over multiple adjacent pixels, only one single m-tube will be counted.[21] In the tested areas of PFBP-SWCNT network, at least one metallic tube existed. Similarly, in the case of F8T2-SWCNT network, two obvious peaks centered at 157 and 163 cm^{-1} emerged (Figure 2h), indicating that there were at least two kinds of metallic tubes detected in the deposited network. However, with respect to PCz-SWCNT network, no characteristic metallic peaks were observed in all the spectra (Figure 2c). To further confirm this observation, we randomly chose and

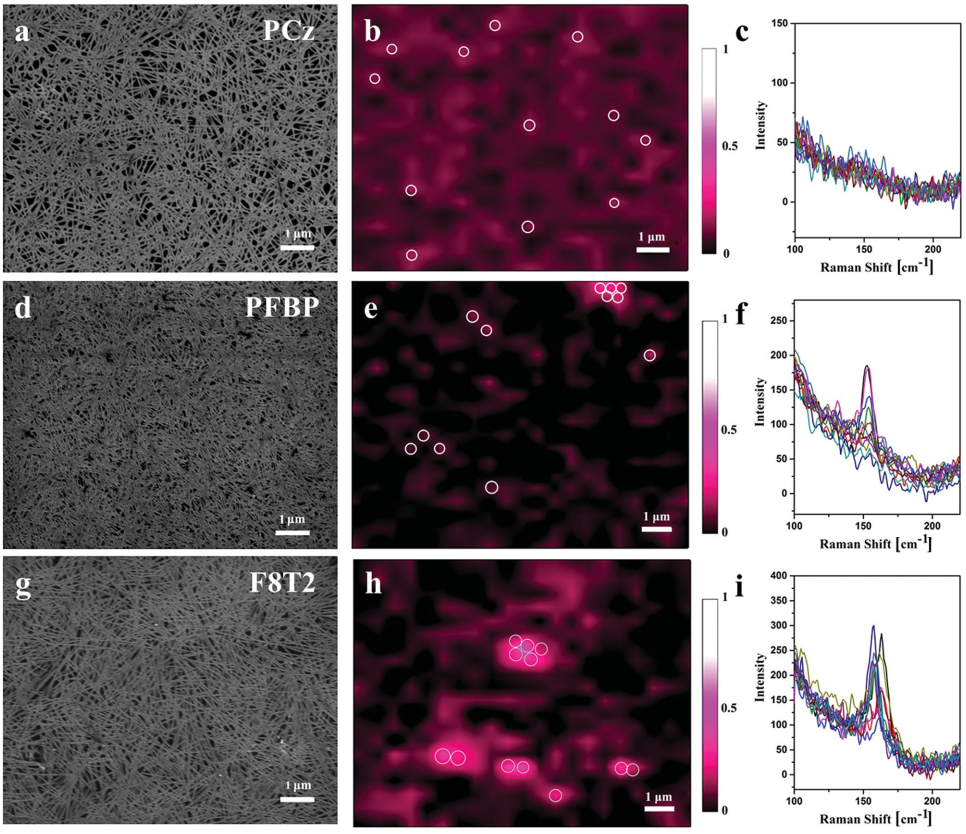

Figure 2. Scanning electronic microscopy (SEM) images of SWCNTs networks prepared by submerging the substrate in the a) PCz-, d) PFBP-, g) F8T2-SWCNTs solution. RBM mapping of b) PCz, e) PFBP, h) F8T2 obtained from integrated intensities in the 130–180 cm^{-1} range and the tested areas are same as in corresponding SEM images. Circles in (b), (e), and (h) highlight positions from which spectra were taken in (c), (f), and (i). Scanned area was 10×10 μm^2 and scale bar is 1 μm.

www.MaterialsViews.com

measured more than ten different areas of the PCz-CNT films, and no metallic signal was found either (Figure S3, Supporting Information). As a result, we concluded that PCz was an excellent dispersant for harvesting the s-SWCNTs with higher purity.

Spectroscopy is hard to be available and accurate enough to characterize the s-SWCNTs with purity higher than 99%. To further quantify the purity, TFT devices with channel length of 500 nm and a width (W) of 2 μm were fabricated on SiO_2 (300 nm)/Si substrate (**Figure 3**a). The purity of s-SWCNTs could be evaluated by measuring on–off ratios of the TFTs and counting the number of tubes spanning TFTs.[14a] Since the length of the sorted s-SWCNTs was in the range of 1–2 μm, we assumed that majority of the sorted s-SWCNTs tend to directly span over the electrode channels. If there were one metallic tube, the devices used would be short-circuited easily. 36 devices with same channel were fabricated and measured, only one device shows an on–off ratio less than 10^2 (Figure 3c and Figure S4a (Supporting Information)), more likely indicating the presence of m-SWCNTs. In addition, the devices with channel length of 500 nm were also characterized at different V_{DS} (–0.1, –1, –5 V), with all on–off ratios kept above 10^4 at a higher bias voltage (Figure S4b, Supporting Information). The atomic force microscope (AFM) image in Figure 3b indicates that more than 25 tubes exist in a 1 μm profile line, and a TFT with channel width of 2 μm can be estimated containing at least 50 SWCNTs. Thus, there are more than 1800 tubes directly span over the channel, indicating that the concentration of metallic impurities is above one part per 1800. As a result, the purity of the sorted s-SWCNTs by PCz can be estimated as high as 99.9%.[14a,23] Because the thickness of SiO_2 dielectric layer is 300 nm, a higher gate voltage is required to control the on- or off-current (from 80 to –80 V). Figure 3d is the output curve of a typical device, it is indicated that the top-contact electrode between palladium and the s-SWCNTs confirms a good ohmic or near-ohmic contact even without PCz removal.

Fabrication of wafer scale and uniform TFTs with high performance is necessary for practical applications. The homogeneity and reliability of the as-fabricated TFT devices may be influenced by a few factors, at least including structural variation (diameter and chirality distribution) of s-SWCNTs, density and uniformity control of as-deposited networks, suitable contact electrode materials and fabrication procedure, etc. In order to obtain the s-SWCNT film with large area and controllable density, SiO_2 surface was treated with hexamethyl disilazane, guaranting the PCz-sorted s-SWCNTs with good wettability on surface. Being placed a Si wafer in sorted s-SWCNT solution for 12 h, the s-SWCNTs tend to deposit into dense and uniform network (as shown in Figure S5, Supporting Information). 240 TFTs with different channel length from 5 to 50 μm and W/L ratios from 2 to 20 were fabricated on a 2 in. SiO_2/Si wafer (**Figure 4**a). The bottom-gate/bottom-contact configuration was used to verify the quality of the as-fabricated devices (Figure 4b). In Figure 4c, the transfer curves of 15 TFTs with channel length and width set at 20 and 400 μm showed high uniformity.

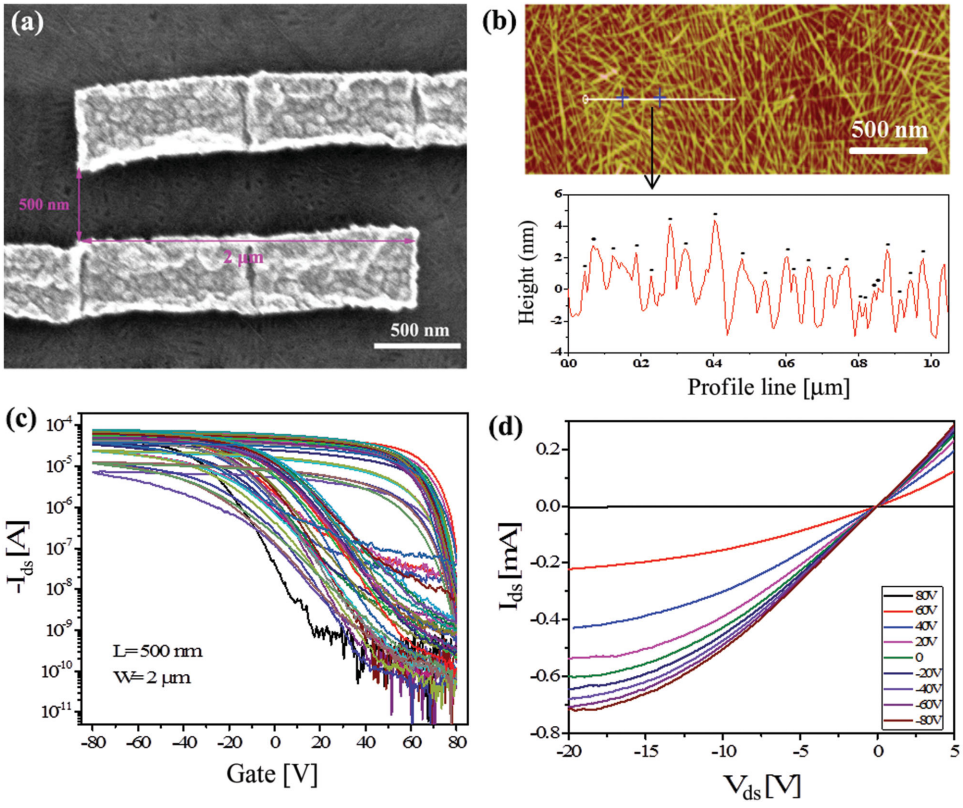

Figure 3. a) SEM image of TFT with nanometer channel. b) AFM image of PCz-dispersed SWCNT network and a typical height line profile to show the tube density in the channel. c) The typical transfer curves of 35 devices and d) the output curves of TFT devices with L = 500 nm and W = 2 μm.

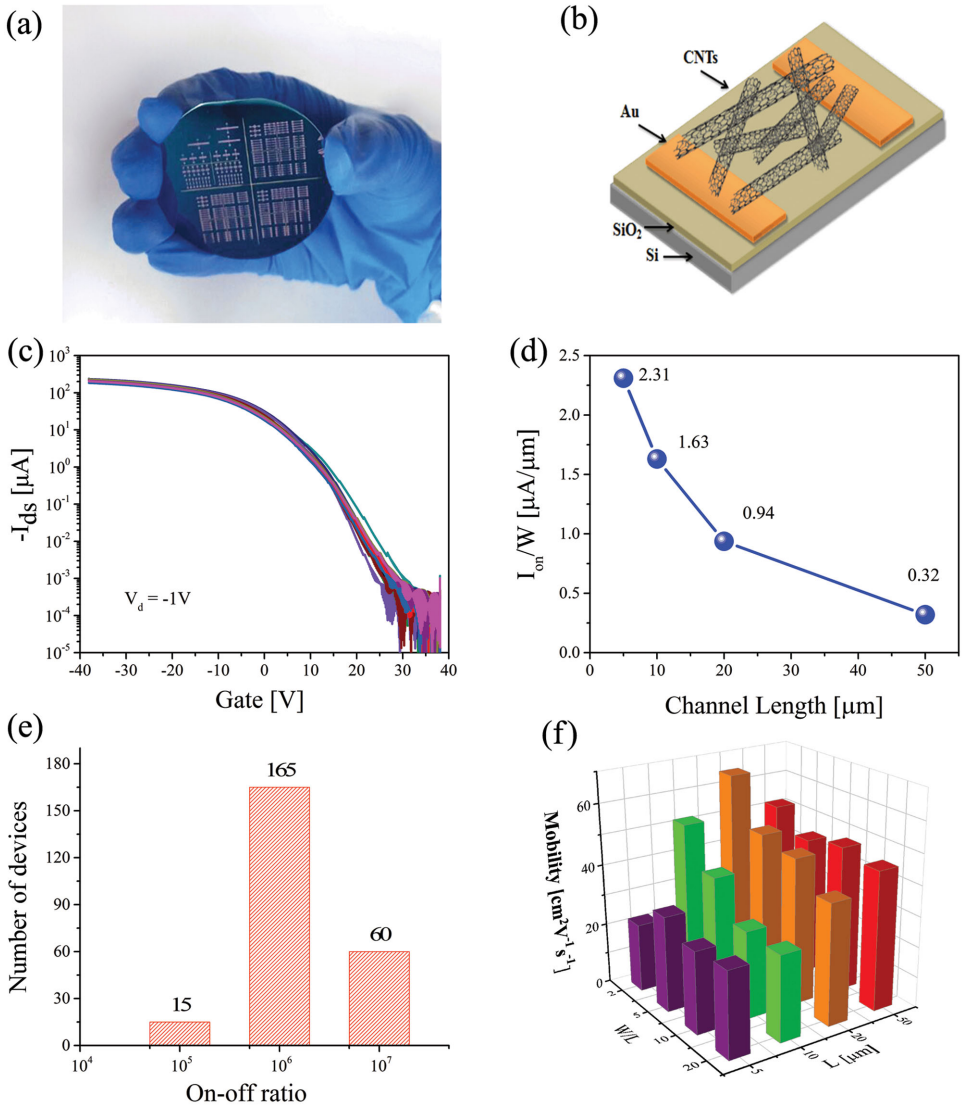

Figure 4. a) The 300 TFTs in a 2 in. N-doped silicon wafer with 300 nm silicon dioxide. b) The structure of bottom-contact TFTs. c) The transfer curves of 15 devices with channel length of 20 μm and a width of 400 μm (V_d = –1 V). d) I_{on} per width versus different channel lengths (V_{DS} = –40 V). e) The on–off ratio and f) mobility distribution of 240 devices with channel length from 5 to 50 μm.

However, its output curve displayed a little reversed bending at V_d < 5 V, indicating a larger contact resistance between s-SWCNTs and Au electrodes (Figure S6, Supporting Information). The contact resistance for the TFTs is calculated to be 91.7 kΩ using the transfer length method. Figure 4d illustrates the dependence of the current density of the devices on channel length varying from 5 to 50 μm. It is seen clearly that the on-current density tends to be inversely proportional to the channel length. The highest on-current density is achieved at 2.33 μA μm^{-1} with the channel length of 5 μm. All of the as-fabricated TFTs exhibited good and reliable performance (Figure S7, Supporting Information). Figure 4e shows the statistical results on the on–off ratios derived from 240 TFTs with channel length varying from 5 to 50 μm at V_d = –1 V. all of the TFTs displayed on–off ratios in a close range from 10^5 to 10^6. Their mobilities were distributed from 28 to 67.5 cm^2 V^{-1} s^{-1}, indicating the sorted s-SWCNTs by PCz were more favorable than other widely used conjugated polymers for wafer-scale fabrication of TFTs. Moreover, for the fabrication of such devices, a larger channel length tended to favor the devices with a higher mobility (Figure 4f), suggesting that the contribution of contact resistance in the total resistance became severe when the devices were fabricated with short channel lengths. Therefore, to solve contact resistance would be another important issue for s-SWCNT based TFT devices.

In summary, we designed and synthesized a polycarbazole (PCz), which showed extraordinary selectivity on the sorting of high purity s-SWCNTs compared to other polyfluorene derivatives. Both spectroscopic characterization and short-channel TFT device measurements confirmed the purity of the sorted s-SWCNTs by PCz as high as 99.9%. The high-purity s-SWCNT solution was scalable and processable for facile fabrication of large-area thin films and TFTs with good uniformity. It is demonstrated that among tens of as-fabricated TFTs on a SiO_2/Si wafer, the transistors exhibited

mobilities of 28–67.5 $cm^2 V^{-1} s^{-1}$ and on–off ratios of 10^5–10^6 when the channel length was fabricated from 5 to 50 μm. As a result, PCz may serve as a promising dispersant for scalable preparation of high-purity s-SWCNT solutions and provide significant opportunities for large-area fabrication of TFTs and the development of complex integrated circuit in near future.

Experimental Section

Materials: Raw Arc-discharged SWCNTs were purchased from Carbon Solution Inc. PFO, F8T2, PFBP, and two monomers (N-9′-heptadecanyl-2,7- dibromocarbazole and 2,7-bis(4′,4′,5′,5′-tetramethyl-1′,3′,2′-dioxaborolan-2′-yl)- N-heptadecanylcarbazole) were purchased from Derthon Optoelectronics Materials Science Technology Co. The 9-(1-octylonoyl)-9H-carbazole-2, 7-diyl (PCz) was prepared by Suzuki polycondensation in relatively high yield (more details in the Supporting Information).

Preparation of SWCNTs: Dispersants PCz, PFO, F8T2, and F8BT (3 mg) and SWCNTs (1.5 mg) were mixed in toluene (6 mL). The solutions were ultrasonicated with a top-tip dispergator (Sonics VC500) for 30 min at an amplitude level of 30%, and then were centrifuged at 20 000 g for 1 h (Allegra X-22R centrifuge) to remove the bundles and insoluble materials. The supernatants were collected for characterization and fabrication of TFTs.

SWCNT Structure Characterization: Optical absorption were measured in 2 mm path length quartz cells by Perkin Elmer Lambda 750 UV–vis–NIR specrometer. Resonance Raman spectra mappings were performed on a Lab Ram HR-800 Raman system from Horiba Jobin Yvon at 785 nm excitation. The SEM images were taken by using S4800 field-emission instrument from Hitachi, Japan. AFM images were taken using tapping mode with Veeco Dimension 3100 AFM.

Fabrication of SWCNT TFTs: Lithographic process was used to fabricate the source/drain patterns, followed by oxygen plasma to etch the residual photoresist. Electron beam evaporation of titanium/gold (4/50 nm) was used to create bottom contacts to the SWCNTs. Dip-coating method was used to fabricate the large-area uniform s-SWCNT film. A second lithographic process was used to define the channel and the exposed s-SWCNTs were removed with oxygen plasma (more details of the calculation methods of mobility and contact resistance in the Supporting Information).

Supporting Information

Supporting Information is available from the Wiley Online Library or from the author.

Acknowledgements

J.G. and J.H. contributed equally to this work. This research was generously supported by National Natural Science Foundation of China (Grant Nos. 61274130 and 21373262).

[1] a) A. D. Franklin, *Science* **2015**, *349*, 704; b) S. J. Tans, A. R. M. Verschueren, C. Dekker, *Nature* **1998**, *393*, 49; c) A. Javey, J. Guo, Q. Wang, M. Lundstrom, H. Dai, *Nature* **2003**, *424*, 654; d) A. D. Franklin, M. Luisier, S.-J. Han, G. Tulevski, C. M. Breslin, L. Gignac, M. S. Lundstrom, W. Haensch, *Nano Lett.* **2012**, *12*, 758; e) A. D. Franklin, *Nature* **2013**, *498*, 443.

[2] a) Q. Cao, H.-s. Kim, N. Pimparkar, J. P. Kulkarni, C. Wang, M. Shim, K. Roy, M. A. Alam, J. A. Rogers, *Nature* **2008**, *454*, 495; b) C. Wang, J. C. Chien, K. Takei, T. Takahashi, J. Nah, A. M. Niknejad, A. Javey, *Nano Lett.* **2012**, *12*, 1527.

[3] a) S. Nanot, A. W. Cummings, C. L. Pint, A. Ikeuchi, T. Akiho, K. Sueoka, R. H. Hauge, F. Leonard, J. Kono, *Sci. Rep.* **2013**, *3*, 1335; b) R. Lu, C. Christianson, A. Kirkeminde, S. Ren, J. Wu, *Nano Lett.* **2012**, *12*, 6244; c) M. E. Itkis, F. Borondics, A. Yu, R. C. Haddon, *Science* **2006**, *312*, 413.

[4] a) D. Lee, T. Cui, *Biosens. Bioelectron.* **2010**, *25*, 2259; b) E. Artukovic, M. Kaempgen, D. S. Hecht, S. Roth, G. Grüner, *Nano Lett.* **2005**, *5*, 757.

[5] a) Z. Jialu, W. Chuan, Z. Chongwu, *ACS Nano* **2012**, *6*, 7412; b) T. Takenobu, T. Takahashi, T. Kanbara, K. Tsukagoshi, Y. Aoyagi, Y. Iwasa, *Appl. Phys. Lett.* **2006**, *88*, 033511; c) R. Nima, J. Dheeraj, B. Peter John, *ACS Nano* **2011**, *5*, 8471.

[6] a) S. Zhang, Y. Hu, J. Wu, D. Liu, L. Kang, Q. Zhao, J. Zhang, *J. Am. Chem. Soc.* **2015**, *137*, 1012; b) Y. M. Li, D. Mann, M. Rolandi, W. Kim, A. Ural, S. Hung, A. Javey, J. Cao, D. W. Wang, E. Yenilmez, Q. Wang, J. F. Gibbons, Y. Nishi, H. J. Dai, *Nano Lett.* **2004**, *4*, 317; c) F. Yang, X. Wang, D. Zhang, J. Yang, D. Luo, Z. Xu, J. Wei, J. Q. Wang, Z. Xu, F. Peng, X. Li, R. Li, Y. Li, M. Li, X. Bai, F. Ding, Y. Li, *Nature* **2014**, *510*, 522.

[7] a) F. Lu, M. J. Meziani, L. Cao, Y.-P. Sun, *Langmuir* **2010**, *27*, 4339; b) H. Zhang, B. Wu, W. Hu, Y. Liu, *Chem. Soc. Rev.* **2011**, *40*, 1324; c) M. C. Hersam, *Nat. Nanotechnol.* **2008**, *3*, 387.

[8] M. S. Arnold, A. A. Green, J. F. Hulvat, S. I. Stupp, M. C. Hersam, *Nat. Nanotechnol.* **2006**, *1*, 60.

[9] a) D. H. Shin, J.-E. Kim, H. C. Shim, J.-W. Song, J.-H. Yoon, J. Kim, S. Jeong, J. Kang, S. Baik, C.-S. Han, *Nano Lett.* **2008**, *8*, 4380; b) R. Krupke, F. Hennrich, H. Lohneysen, M. M. Kappes, *Science* **2003**, *301*, 344.

[10] a) T. Tanaka, H. Jin, Y. Miyata, S. Fujii, H. Suga, Y. Naitoh, T. Minari, T. Miyadera, K. Tsukagoshi, H. Kataura, *Nano Lett.* **2009**, *9*, 1497; b) T. Tanaka, Y. Urabe, D. Nishide, H. Kataura, *Appl. Phys. Express* **2009**, *2*, 125002.

[11] a) C. Y. Khripin, J. A. Fagan, M. Zheng, *J. Am. Chem. Soc.* **2013**, *135*, 6822; b) M. S. Y. Tang, T. J. Whitcher, K. H. Yeoh, C. L. Chua, K. L. Woon, P. L. Show, Y. K. Lin, T. C. Ling, *J. Nanosci. Nanotechnol.* **2014**, *14*, 3398.

[12] G. S. Tulevski, A. D. Franklin, A. Afzali, *ACS Nano* **2013**, *7*, 2971.

[13] C. Wang, K. Takei, T. Takahashi, A. Javey, *Chem. Soc. Rev.* **2013**, *42*, 2592.

[14] a) G. J. Brady, J. Yongho, W. Meng-Yin, M. J. Shea, G. Padma, M. S. Arnold, *ACS Nano* **2014**, *8*, 11614; b) F. Hennrich, W. Li, R. Fischer, S. Lebedkin, R. Krupke, M. M. Kappes, *ACS Nano* **2016**, *10*, 1888.

[15] a) S. K. Samanta, M. Fritsch, U. Scherf, W. Gomulya, S. Z. Bisri, M. A. Loi, *Acc. Chem. Res.* **2014**, *47*, 2446; b) J. Ding, Z. Li, J. Lefebvre, F. Cheng, G. Dubey, S. Zou, P. Finnie, A. Hrdina, L. Scoles, G. P. Lopinski, C. T. Kingston, B. Simard, P. R. L. Malenfant, *Nanoscale* **2014**, *6*, 2328; c) N. Berton, F. Lemasson, A. Poschlad, V. Meded, F. Tristram, W. Wenzel, F. Hennrich, M. M. Kappes, M. Mayor, *Small* **2014**, *10*, 360.

[16] a) W. Gomulya, G. D. Costanzo, E. J. de Carvalho, S. Z. Bisri, V. Derenskyi, M. Fritsch, N. Frohlich, S. Allard, P. Gordiichuk, A. Herrmann, S. J. Marrink, M. C. dos Santos, U. Scherf, M. A. Loi, *Adv. Mater.* **2013**, *25*, 2948; b) F. Chen, B. Wang, Y. Chen, L.-J. Li, *Nano Lett.* **2007**, *7*, 3013; c) A. Nish, J.-Y. Hwang, J. Doig, R. J. Nicholas, *Nat. Nanotechnol.* **2007**, *2*, 640.

[17] K. S. Mistry, B. A. Larsen, J. L. Blackburn, *ACS Nano* **2013**, *7*, 2231.
[18] a) Z. Chen, J. Appenzeller, J. Knoch, Y. M. Lin, P. Avouris, *Nano Lett.* **2005**, *5*, 1497; b) W. Kim, A. Javey, R. Tu, J. Cao, Q. Wang, H. Dai, *Appl. Phys. Lett.* **2005**, *87*, 173101.
[19] J.-F. Brière, M. Côté, *J. Phys. Chem. B* **2004**, *108*, 3123.
[20] a) W. Xu, J. Zhao, L. Qian, X. Han, L. Wu, W. Wu, M. Song, L. Zhou, W. Su, C. Wang, S. Nie, Z. Cui, *Nanoscale* **2014**, *6*, 1589; b) J.-F. Brière, M. Côté, *J. Phys. Chem. B* **2004**, *108*, 3123.
[21] Z. Li, J. Ding, P. Finnie, J. Lefebvre, F. Cheng, C. T. Kingston, P. R. L. Malenfant, *Nano Res.* **2015**, *8*, 2179.
[22] P. Finnie, J. Ding, Z. Li, C. T. Kingston, *J. Phys. Chem. C* **2014**, *118*, 30127.
[23] T. Lei, X. Chen, G. Pitner, H. P. Wong, Z. Bao, *J. Am. Chem. Soc.* **2016**, *138*, 802.

Received: February 4, 2016
Revised: March 29, 2016
Published online: April 26, 2016